Increased EEG power and slowed dominant frequency in patients with neurogenic pain

Johannes Sarnthein,[1,2] Jair Stern,[1] Christoph Aufenberg,[1] Valentin Rousson[3] and Daniel Jeanmonod[1,2]

[1]Universitätsspital, Funktionelle Neurochirugie, CH-8091 Zürich, [2]Center for Integrative Human Physiology and [3]Biostatistik, Universität Zürich, Switzerland

Correspondence to: Johannes Sarnthein, Funktionelle Neurochirurgie, Universitätsspital, CH-8091 Zürich, Switzerland
E-mail: johannes.sarnthein@usz.ch

To study the mechanisms of chronic neurogenic pain, we compared the power spectra of the resting EEG of patients (n = 15, 38–75 years, median 64 years, 6 women) and healthy controls (n = 15, 41–71 years, median 60 years, 8 women). On an average, the patient group exhibited higher spectral power over the frequency range of 2–25 Hz, and the dominant peak was shifted towards lower frequencies. Maximal differences appeared in the 7–9 Hz band in all electrodes. Frontal electrodes contributed most to this difference in the 13–15 Hz band. Bicoherence analysis suggests an enhanced coupling between theta (4–9 Hz) and beta (12–25 Hz) frequencies in patients. The subgroup of six patients free from centrally acting medication showed higher spectral power in the 2–18 Hz frequency range. On an individual basis, the combination of peak height and peak frequency discriminated between patient and control groups: discriminant analysis classified 87% of all subjects correctly. After a therapeutic lesion in the thalamus (central lateral thalamotomy, CLT) we carried out follow-up for a subgroup of seven patients. Median pain relief was 70 and 95% after 3 and 12 months, respectively. The average EEG power of all seven patients gradually decreased in the theta band and approached normal values only after 12 months. The excess theta EEG power in patients and its decrease after thalamic surgery suggests that both EEG and neurogenic pain are determined by tightly coupled thalamocortical loops. The small therapeutic CLT lesion is thought to initiate a progressive normalization in the affected thalamocortical system, which is reflected in both decrease of EEG power and pain relief.

Introduction

While several mechanisms have been proposed for the pathophysiology of neurogenic pain (Treede *et al.*, 1999; Peyron *et al.*, 2000; Jones *et al.*, 2003; Apkarian *et al.*, 2005) no general agreement has been reached yet. In the following we refer to a mechanism that focuses on thalamocortical interplay (Llinás *et al.*, 1999). First evidence for this mechanism was the finding of low-threshold calcium spike (LTS) bursts in the somatosensory thalamus of patients with neurogenic pain (Lenz *et al.*, 1989). A detailed investigation (Jeanmonod *et al.*, 1993) in the medial thalamus (central lateral nucleus, CL) showed that (i) half of all recorded neurons presented LTS bursting activity, (ii) only a minority (<1%) had somatosensory receptive fields and (iii) LTS bursts displayed a theta rhythmicity, with a mean interburst discharge rate of 4 Hz. LTSs have been described intracellularly in *in vitro* and *in vivo*

experiments and have been related to a state of membrane hyperpolarization (Llinás and Jahnsen, 1982; Steriade, 2001). CL is part of the medial thalamus, is diffusely connected to wide cortical areas (Steriade *et al.*, 1997; Jones, 2001) and is thought to serve as the non-specific amplifier of thalamocortical activity (Llinas *et al.*, 2002). Functionally, the tight coupling of the thalamocortical re-entry loop is reflected by high thalamocortical coherence in human patients (Sarnthein *et al.*, 2003). This loop constitutes an important component contributing to the rhythmicity of scalp EEG and magnetoencephalography (MEG) (Nunez *et al.*, 2001). Furthermore, slowed EEG/MEG rhythmicity has been reported in a few patients with neurogenic pain (Gücer *et al.*, 1978; Llinás *et al.*, 1999; Sarnthein *et al.*, 2003). Based on these physiological findings and the clinical fact that a therapeutic

lesion in CL (central lateral thalamotomy, CLT) relieves pain and other functional brain disorders (Jeanmonod *et al.*, 1993, 1996, 2001*a*), thalamocortical dysrhythmia (TCD) was proposed as a general mechanism to explain the generation of neurogenic pain and other positive neurological symptoms (Llinás *et al.*, 1999, 2001; Jeanmonod *et al.*, 2001*b*). However, the pioneering reports of slowed EEG/MEG rhythmicity in neurogenic pain were related to only a small number of patients.

The present study aimed, first, to discriminate statistically between neurogenic pain patients and healthy controls on the basis of scalp EEG spectral parameters. Second, we hypothesized a theta reduction in patients' EEG after the surgical intervention CLT, which has the goal to reduce thalamic LTS production. We therefore monitored the EEG 3 and 12 months after the therapeutic lesion.

Methods
Patients
The patient group consisted of 17 patients with severe forms of neurogenic pain that fulfilled all admission criteria for CLT neurosurgical therapy (see below). Following the terminology of the International Association for the Study of Pain, we use the term neurogenic pain to refer to the pain initiated or caused by a primary lesion, dysfunction, or transitory perturbation in the peripheral or central nervous system. Of the initial patient group, we excluded one patient due to eye movement artefacts in the EEG and one patient because of low voltage EEG. Symptoms, medication and pain relief reported by the remaining patients in the group (n = 15, 38–75 years, median 64 years, 6 women, 9 men) are listed in Table 1. After surgery, three patients died due to unrelated reasons, two were not available for EEG and three await EEG follow-up to date. Therefore, a subgroup of n = 7 patients was available for recording EEG at 3 and 12 months after surgery.

Surgery
Neurosurgical therapy for the patients consisted of CLT, a therapeutic lesion in the posterior part of the thalamic nucleus, CL (Morel *et al.*, 1997), and has been described in detail previously (Jeanmonod *et al.*, 2001*a*). Admission criteria for CLT include resistance to drug therapies (antiepileptics, benzodiazepines and antidepressants), chronic pain state >1 year, severe suffering and a strongly diminished quality of life. Distinct from all other lesional procedures applied in chronic pain, CLT targets cells in the posterior part of CL which have been found to be functionally blocked. Therefore the normal functions of CL are spared by CLT, since they have been transferred to other areas by plastic reorganization of the thalamocortical network. In a previous study with n = 96 patients and a follow-up of 4 years, >50% of the patients obtained pain relief (satisfactory up to complete relief) (Jeanmonod *et al.*, 2001*a*).

Healthy controls
The healthy control group consisted of 15 subjects (41–71 years, median 60 years, 8 women, 7 men). The control subjects had no current or previous history of relevant physical illness and they were not currently taking drugs or medication known to affect their EEG. The healthy, age-matched control group was selected to statistically delineate the EEG abnormality reported in a small number of patients (Gücer *et al.*, 1978; Llinás *et al.*, 1999; Sarnthein *et al.*, 2003). Furthermore, the healthy control group served as a reference when postoperative changes in the patients EEG were monitored.

EEG recording sessions
The study was approved by the Kanton Zürich ethics committee. All subjects, patients and controls, were informed about the aim and the scope of the study and all gave written informed consent according to the Declaration of Helsinki. Subjects were seated in a dimly lit room shielded against sound and stray electric fields and were video-monitored. All EEGs were acquired in the morning between 9 and 12 h. Recording sessions of patients and controls were followed by an interleaved schedule and the recording apparatus was continuously calibrated. Subjects refrained from caffeinated beverages before the session to avoid the caffeine-induced theta decrease in EEG (Landolt *et al.*, 2004). Since drowsiness may result in enhanced theta power, the vigilance of subjects was checked. In addition, patients were routinely asked whether they had sleeping disorders because insomnia conflicts with the typical clinical diagnosis of neurogenic pain.

Within each session, spontaneous EEG was recorded under two conditions: while subjects rested with their eyes closed, and while they rested with their eyes open. EEG was recorded for 5 min under each condition. We focused our analysis on the eyes closed condition as it is less prone to artefacts and we assume that an internal process like neurogenic pain should be more easily accessed in the brain's 'idling mode' (Pfurtscheller *et al.*, 1996), unmasked by sensory perception. Therefore all results presented in this study refer to the eyes closed condition, except for Fig. 1D. We refrained from provoking acute pain since we are interested in the pathophysiology of chronic neurogenic pain that is experienced independent of nociceptive stimuli. Before each recording segment, subjects were instructed to assume a comfortable position in a chair. They were free to place their head on a chin-rest. For the eyes closed condition, subjects were instructed to close their eyes, to place their fingers on their eyelids, and to relax but to stay awake. After 5 min subjects were instructed to open their eyes, to fixate on a dot at 1 m distance and to relax.

EEG signals were measured using 60 Ag/AgCl surface electrodes, which were fixed in a cap at the standard positions according to the extended 10–20 system (FMS11, Falk Minow Services, Herrsching, Germany). Electrode CPz served as the common reference. Impedances were below 5 kΩ in all electrodes processed in the further analysis. We used two additional bipolar electrode channels as eye monitors. EEG signals were registered using the SynAmps EEG system (Neuroscan Compumedics, Houston, TX, 16 bit A/D conversion, sampling rate 250 Hz, 0.3–100 Hz band pass filter, −12 dB/octave) and continuously viewed on a PC monitor.

Data preprocessing and editing
Data were analysed offline using Matlab (The Mathworks, Natick, MA) using EEGLAB (http://sccn.ucsd.edu/eeglab; Delorme and Makeig, 2004) and custom scripts. The scalp EEG was re-referenced to the mean of the signals recorded at the ear lobes. We confirmed alertness of subjects during the recording session by checking for slowing of the alpha rhythm, slow rolling eye movements or increasing theta power (4–9 Hz). Data were inspected in 5 s epochs, and large muscle

Table I Clinical description of individual patients

Patient							Preoperative		Surgery target	3 months		12 months	
No.	Age	Sex	Pain location	Pain side	Pain type/cause	Lesion level	VAS	Drugs (%)		Relief	Drugs (%)	Relief	Drugs (%)
1	75	F	Trigeminal	Right	co,al,ep/herpes	p	75	BZ	CLT lr	100	–	100	–
2	68	M	Trigeminal	Right	co,al,ep,pa/tumour	p	60	–	CLT lr	80	>AE	95	–
3	38	M	Trigeminal	Right	al,ep,pa/tumour	p	70	AE, AD	CLT ri	50	BZ, AD, >OP	95	>BZ, AD
4	51	F	Trigeminal	Right	co,al,ep,pa/idiopathic	p	50	BZ, AD, OP	CLT le	100	>AE, BZ	100	–
5	66	M	Trigeminal	Right	al,pa/vascular	c	100	AE, OP	CLT ri				
6	69	F	Trigeminal	Right	co,al,pa/idiopathic	p	75	BZ, AD	CLT ri				
7	73	M	Trigeminal	Left	co,pa/tumour	c	63	BZ, AD	CLT le				
8	62	M	Leg	Right	co/trauma	p	60	–	CLT le				
9	58	F	Leg	Left	co,ep/root lesion	p	73	AE, BZ, AD, OP	CLT ri	25	>AE,BZ, AD,OP	95	>BZ, AD
10	54	F	Leg	Left	co/root lesion	p	65	–	CLT ri	70	–	75	–
11	64	M	Leg	Left	co/trauma	p	60	–	CLT le				
12	68	M	Leg	Left	co,al,ep/spinal cord lesion	c	80	–	CLT ri				
13	73	F	Hemibody	Left	co/vascular	c	65	–	CLT ri	0	<AE, AD, >OP	0	>AE, BZ
14	52	M	Cervical	Right	co,ep/tumour/neurectomy	p	60	AE, BZ,OP	CLT le				
15	61	M	Arm	Both	co,al/polyneuropathy	p	75	AE, AD, OP	CLT lr				
Median pain relief										70		95	

Pain locations are trigeminal, lower limb (leg), hemibody, cervical, and upper limb (arm). Pain types are constant (co), allodynic (al), episodic (ep) and paroxysmal (pa). Lesion levels are central (c) and peripheral (p). Pain intensity was rated on a visual analogue scale (VAS) in %. Displayed are mean VAS ratings and, in the absence of constant pain, the VAS rating during pain attacks. Relevant drugs include antiepileptics (AE), benzodiazepines (BZ), antidepressants (AD) and opiates (OP). Surgical targets were CLT left (le), CLT right (ri), or CLT left and right (lr). Postoperative development was characterized by decrease (<) or increase (>) in drug dose and percentage of pain relief (%).
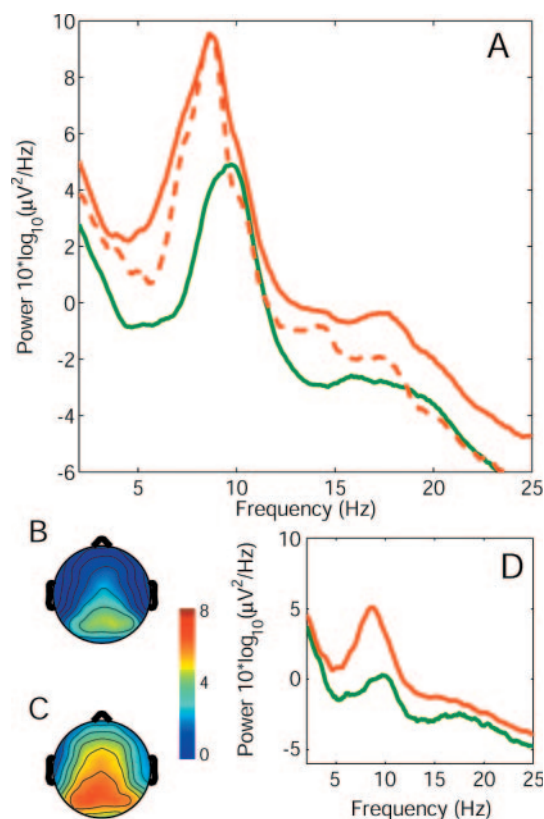
Fig. 1 Average power spectra. The spectrum for the group of patients (red) and the group of healthy controls (green) with eyes closed (**A**). The global EEG power was enhanced in patients and the dominant peak was shifted towards lower frequencies in the patient population. The subgroup of six patients free from centrally acting medication showed the same effect in the 2–18 Hz frequency range (**A**, dashed line). The topographical distribution of EEG power (5–13 Hz, eyes closed) on the scalp of control group (**B**) and patient group (**C**) had a maximum at parietal electrode sites, but extended to more frontal regions in the patient group. (**D**) Upon opening the eyes, the power spectral density was reduced in both the groups, but theta overactivity persisted in the patient group.

or eye movement artefacts were removed. For editing purposes, muscle artefact was considered significant if the underlying EEG rhythms were not clearly seen. The EEG was decomposed into independent components using blind separation (independent component analysis). After the removal of components containing eye movement or muscle artefacts, the signal was reconstructed. This procedure resulted in >60 s of EEG for estimates of power spectral density (mean 244 ± 50 s). For the analysis of inter-frequency relationships, a stretch of >20 s EEG was selected where power spectra remained unchanged over time (mean 150 ± 86 s). All records were edited using the same encephalographer in order to increase reliability.

Data analysis

For power spectral density estimates, the multitaper FFT method was applied to 5 s windows with $K = 3$ tapers and a bandwidth parameter $2W = 0.8$ Hz, leading to a time bandwidth product $2WT = 4$ (Percival and Walden, 1993). In the comparisons between spectral parameters,

all P values are two-sided from non-parametric Wilcoxon tests. Wherever necessary, EEG spectra were subdivided into frequency bands theta (4–9 Hz), alpha (9–12 Hz), beta (12–25 Hz) and gamma (25–100 Hz). In order to summarize the data and because spectra from all electrodes had similar shape and scale, we averaged the log-transformed spectra of all scalp electrodes for each subject if not stated otherwise.

In order to classify individual subjects into patients and controls on the basis of EEG parameters, classical linear discriminant analyses were carried out. That is, we were seeking for the linear combination of the parameters that best separated the two groups in the sense that it maximized the 'between-to-within' variance ratio. Each subject was then assigned to the closest group based on this linear combination. For this step, cross-validation has been used (SPSS version 11.5) such that the chance level of assigning a subject to the correct group was 50%. Exact 95% confidence intervals for the true proportions of correct classification using EEG parameters were calculated from tabulated values for the binomial distribution and we could check whether the chance level 50% was within or outside these confidence intervals.

To learn about the relationship between power at two frequencies f_1 and f_2 in one EEG signal, we computed bicoherence for each electrode separately. Bicoherence estimates the second-order phase coupling by normalizing the bispectrum $B(f_1, f_2) = \langle X(f_1) \; X(f_2) \; X^*(f_1 + f_2) \rangle$ such that bicoherence is confined to $[0 \; 1]$, where $X(f_1)$ is the complex Fourier transform of the signal at frequency f_1 (Schack *et al.*, 2002). Bicoherence provides phase information as additional information beyond the power spectrum.

Results
Slowed EEG rhythmicity

As a first result, Fig. 1A shows a clear difference between the average power spectra in the resting EEG of the patient group and the healthy control group. In the patient group, spectral power was higher than in the control group over the whole frequency range (2–25 Hz), and the dominant peak was shifted towards lower frequencies. The subgroup of six patients free from centrally acting medication showed the same effect in the 2–18 Hz frequency range (Fig. 1A, dashed line). The scalp topographical distribution of EEG power at the dominant frequency was maximal in posterior electrodes (Fig. 1B and C). This was expected since subjects had their eyes closed (Berger, 1930; Nunez *et al.*, 2001). In the patient group the region of high power extended to more fronto-central electrodes (Fig. 1C). In both patient and control groups, the dominant peak of the EEG was reduced ('blocked') when subjects opened their eyes (Fig. 1D) thus displaying a well-established characteristic of the classical alpha rhythm (Berger, 1930; Pfurtscheller *et al.*, 1996; Nunez *et al.*, 2001; Sarnthein *et al.*, 2005). Nevertheless, also with eyes open the theta overactivity persisted in the patient group.

Individual patients

For each subject the height and the frequency of the dominant peak are plotted in Fig. 2. Patients and controls are given as two separate groups. The power values at the dominant
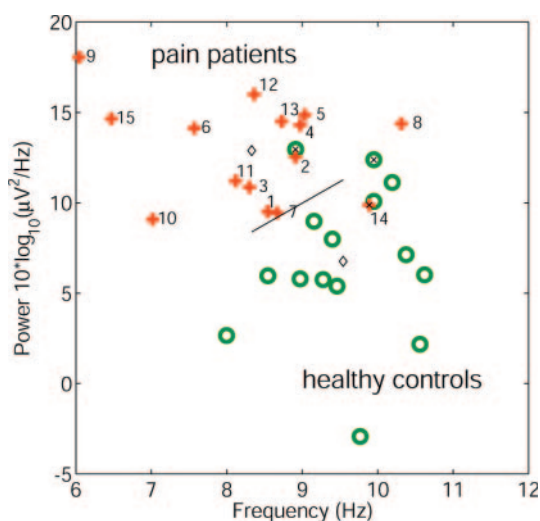
Fig. 2 Individual subject EEG spectral parameters. Height and frequency of the dominant peak for each subject in the patient group (crosses) and the control group (circles). Numbers denote respective patients (Table 1). Using the parameters peak height and peak frequency, bivariate discriminant analysis (group centres: diamonds, misclassified subjects: 'x') classified 87% of all subjects correctly.

frequency come from two distributions with significantly different medians (patients $13.7 \times 10 * \log_{10}(\mu^2/\text{Hz})$, controls $6.2 \times 10 * \log_{10}(\mu^2/\text{Hz})$, $P < 0.0001$, two-tailed Wilcoxon rank sum test). Median dominant frequencies were 8.6 and 9.4 Hz for the patient group and the control group, respectively ($P < 0.002$). Discriminant analysis classified 73% of all subjects correctly based only on peak frequency (95% CI 54–88%), 80% based only on peak height (61–92%) and 87% (69–96%) when both the parameters were accounted for. Since cross-validation was used to estimate the classification rate and all confidence intervals exclude the 50% level (chance level), our results are significant at the 95% level.

Medication and clinical data of the patients are listed in Table 1. Of the 15 patients, 9 took medication known to be centrally acting and which could have affected their EEG (Niedermeyer and Lopes da Silva, 1999; Ebersole and Pedley, 2003). For example, those patients (9, 15) with very high and very slow dominant peak took antiepileptic drugs (AE, Table 1). This is in line with the known effect of AE on EEG, which, however, displays a large inter-individual variability (Salinsky *et al.*, 2003). There are thus two cumulative components, AE effects and neurogenic pain pathophysiology, both of which result in a slowed rhythmicity of the EEG of our patients. Effects of other drugs like antidepressants and opiates could not consistently be related to EEG parameters of individual patients. The effect of neurogenic pain pathophysiology alone is documented by the subgroup of six patients without centrally acting medication (NM). On one hand, the enhanced beta power above 18 Hz seen between the solid red curve (all patients) and the dashed red curve (NM subgroup) in Fig. 1A is compatible with the influence of benzodiazepines (Lindhardt *et al.*, 2001) and may illustrate
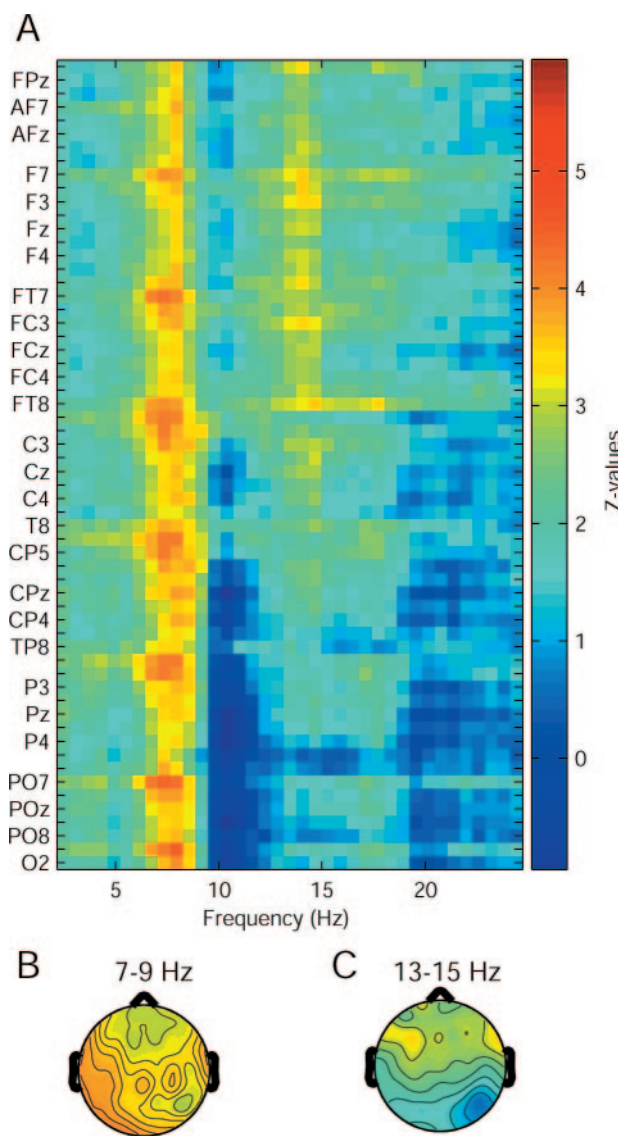

Fig. 3 Comparison of medians of the patient and control groups. (**A**) Shown are Z-values for each electrode and frequency point (Wilcoxon rank sum tests). (**B**) High Z-values occurred from 7–9 Hz in all electrodes. (**C**) Between 13 and 15 Hz, Z-values were maximal in frontal electrodes.

the additive effect of medication and neurogenic pain. On the other hand, the EEG peak parameters of the NM subgroup were well distinct from the healthy control group and the discriminant analysis classified 86% (64–97%) of all subjects correctly.

Topography and frequency dependence

After having established a significant difference between patient group and control group in spectra averaged over all electrodes, we were interested to know which electrodes contributed most to this difference and at what frequency. We performed Wilcoxon rank sum tests for each electrode at each frequency point and plotted the matrix of Z-values as given in Fig. 3A. Maximal Z-values appeared in the 7–9 Hz band in all the electrodes, leading to a rather flat topography (Fig. 3B).

Owing to the alpha peak of healthy controls of ∼10 Hz, Z-values were negative in parietal and occipital electrodes (deep blue area in Fig. 3A). In the 13–15 Hz band, Z-values were high in frontal electrodes (Fig. 3C).
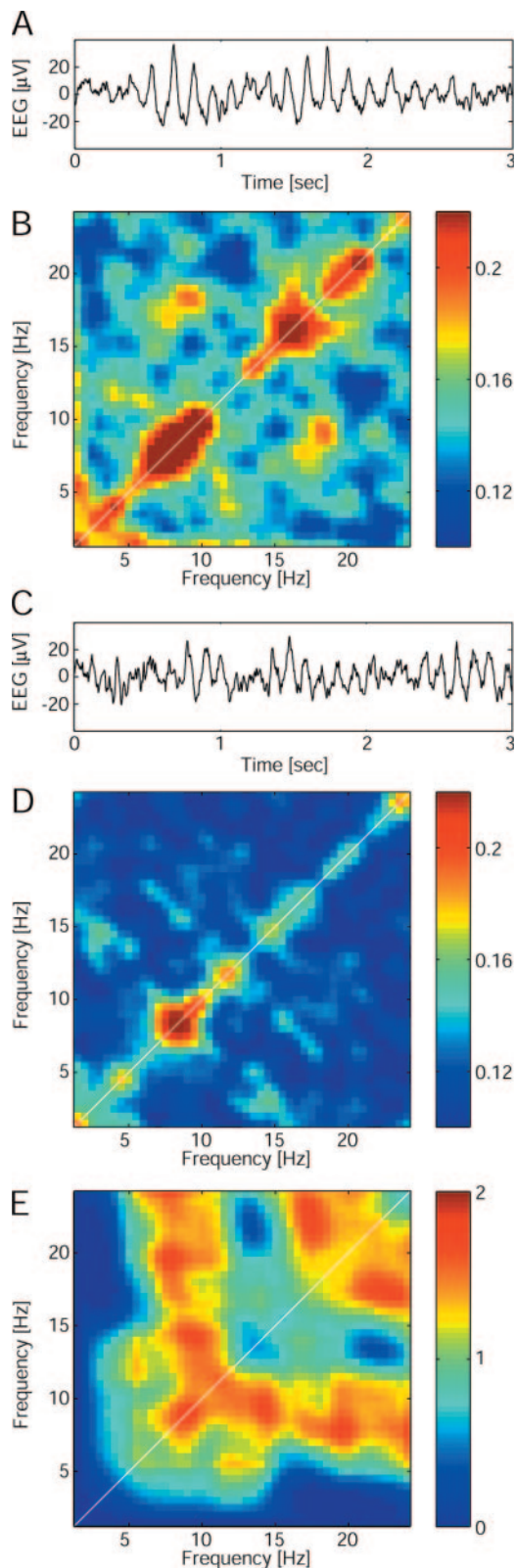
Interfrequency relationships

We next investigated the relationship between different frequencies in the EEG. In patients we found bicoherence maxima in the theta and beta bands at the fronto-central electrode FCz, indicating phase correlations of oscillatory events in these frequency bands with their first harmonic (Fig. 4). Further maxima indicate that phase coupling also occurred between theta and beta frequencies. In healthy controls, less interfrequency relationships were visible (Fig. 4D). In part, the coupling between an oscillation and its overtone can be explained by the triangular shape of the EEG waves at the dominant frequency f. The triangular waveshape is visible in the raw EEG (Fig. 4A) and can lead to a peak at the second harmonic at $2 * f$ in the power spectrum (Dumermuth *et al.*, 1971). The waveshape also explains why power covaries at the fundamental and the overtone frequencies. Patients exhibit higher theta–beta bicoherence at FCz, because the alpha-shaped waves at their dominant frequency extend to more frontal electrodes. Of course triangular waves are common in the EEG of healthy subjects and in themselves not pathological (Niedermeyer and Lopes da Silva, 1999). Only the enhanced occurrence of triangular waves suggests an abnormal coupling between theta and beta frequencies in patients.

Postoperative development

Finally, we were interested in the effect of the therapeutic CLT lesion on the EEG. A subgroup of n = 7 patients was available for EEG recording at 3 and 12 months postoperatively. Of these, one patient reported 0% pain relief and six patients reported immediate or gradually increasing pain relief (median 95%, Table 1). The average EEG spectrum of this patient subgroup gradually approached the average spectrum of the healthy control group (Fig. 5A). In all the patients we also found a gradual decrease in theta power towards the level of the healthy control group (Fig. 5B). Comparison of bicoherence patterns before and 1 year after the surgery showed a reduction of inter-frequency coupling (Fig. 6).

While a postoperative change in theta power could in principle also arise from normal test–retest variability of the EEG (Salinsky *et al.*, 1991), in our group (n = 7) the

Fig. 4 Inter-frequency relationships for the EEG signal recorded at the electrode FCz. (**A**) The raw EEG waveform of patient 10 is asymmetric in the sense that positive peaks are sharper than negative peaks. This triangular waveshape resembles the function $\sin^2(x)$ and results in enhanced second-order phase coupling between the theta band oscillation and its overtone in the beta band for this patient. (**B**) Bicoherence averaged over the patient group shows second-order phase coupling in the diagonal and also between theta and beta bands. (**C**) In the raw EEG waveform of a healthy control, the asymmetry between positive and negative peaks is less pronounced. (**D**) Average bicoherence in the healthy control group lacks off-diagonal peaks. (**E**) Z-values for the comparison between bicoherence maps of the patient group and the healthy control group (Wilcoxon rank sum tests). Bicoherence tends to be higher in patients in the diagonal as well as for theta–beta coupling.
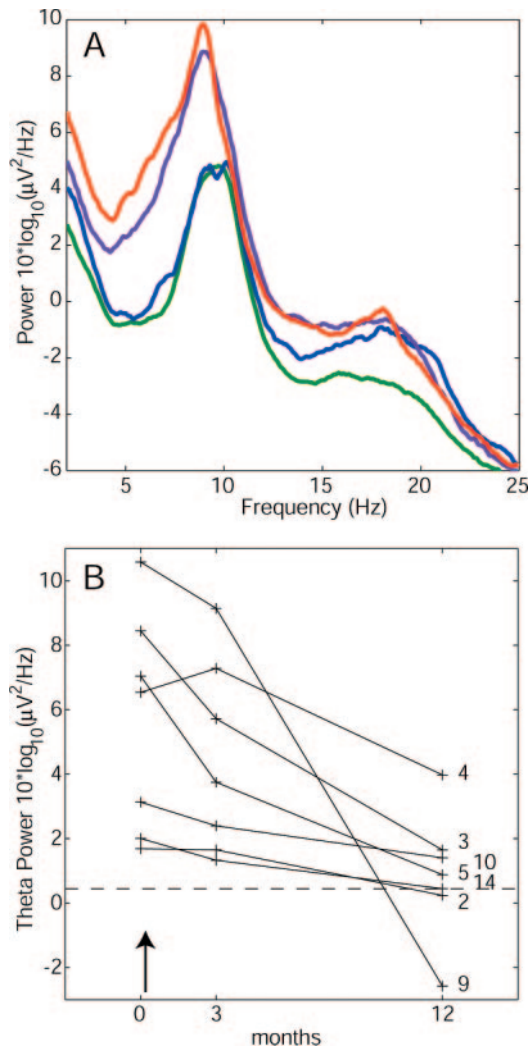
Fig. 5 Reduction of EEG power after the therapeutic lesion CLT. (**A**) The average spectrum of a patient subgroup (n = 7) before surgery (red), after 3 months (violet) and after 12 months (blue) gradually approached that of the healthy control group (green). (**B**) The power level in the theta band (4–9 Hz) is plotted before (months = 0) and after surgery (↑). After 12 postoperative months, theta reduction was observed in all the seven patients ($P < 0.02$). Patient theta levels approached the average of the healthy control group (dashed line).

theta reduction preoperative versus 12 months postoperative is probably related to the surgical intervention ($P < 0.02$, paired Wilcoxon sign rank test). In other frequency bands we observed only insignificant changes. While in three patients (3, 5, 9) the reduction of AE could have contributed to theta reduction (Salinsky *et al.*, 2003), also the two patients without centrally acting medication (2, 10) evidenced a clear reduction of theta postoperatively.

Discussion
Theta dominance in resting EEG

The most obvious characteristic in the EEG spectra of the patient group was the slowing of the dominant peak and

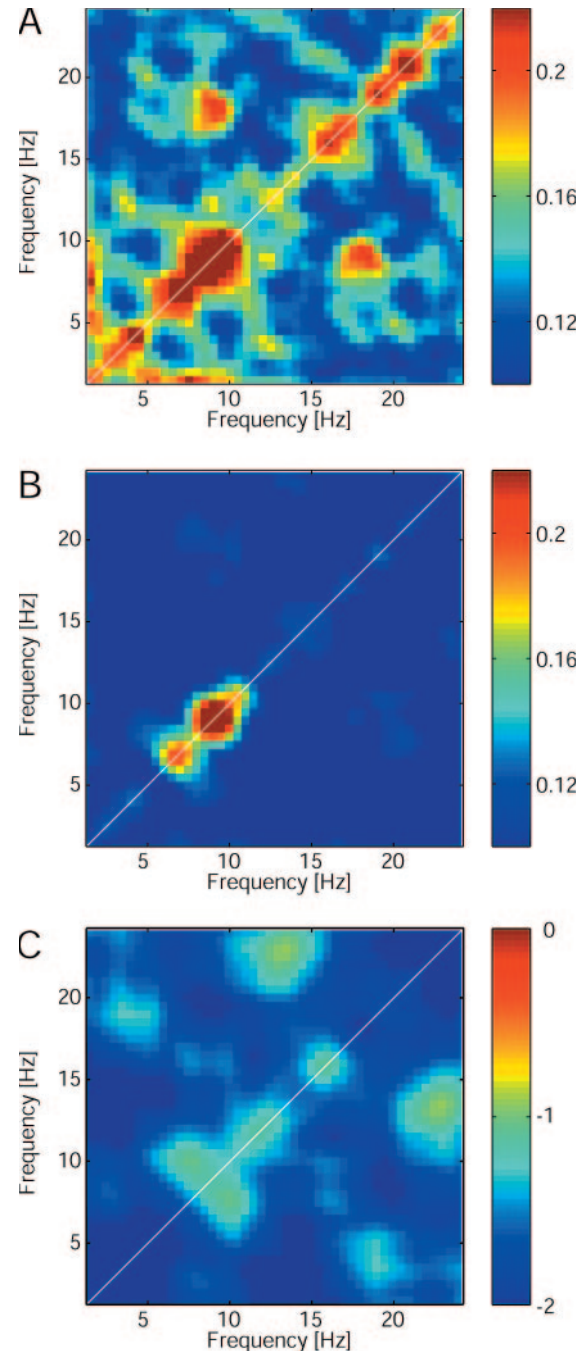**Fig. 6** Reduction of EEG bicoherence at the electrode FCz after the therapeutic lesion CLT. (**A**) Bicoherence values averaged over the patient subgroup (n = 7) before surgery. (**B**) One year after the surgery, off-diagonal peaks were diminished. (**C**) The Z-values for the paired comparison between bicoherence maps (Wilcoxon sign rank tests) show a general decrease of interfrequency coupling in the patient group 1 year after surgery.

enhanced theta and beta power (Fig. 1), in line with previous publications (Gücer *et al.*, 1978; Llinás *et al.*, 1999; Sarnthein *et al.*, 2003). The average peak frequency of the patient group (8.4 Hz) was below the slowed mean EEG peak frequency reported for normal ageing (Niedermeyer and Lopes da Silva, 1999; McEvoy *et al.*, 2001; Ebersole and Pedley,

2003). Both peak height and peak frequency gave the best discrimination between patient group and control group (Fig. 2). In this way we have substantiated the difference in EEG between neurogenic pain patients and healthy controls on a statistical basis. The general slowing and theta over-activity reported in our patients (Fig. 3) correspond to a constantly altered resting EEG and is viewed as an aspect of the pathophysiology. As a result of our selection criteria, pain locations vary among patients. Our results therefore reflect the pathophysiology of neurogenic pain common to all patients. We have refrained from comparisons in sub-groups because of their insufficient size. Finally, our findings might also be related to effects of medication as discussed in the previous section (Table 1). We estimate the effect of medication to be of secondary relevance since theta over-production occurred also in the unmedicated subgroup of six patients.

TCD

The mechanisms generating resting EEG are still a subject of debate, in particular the role of the thalamus (Nunez *et al.*,

2001). Encouraged by our earlier finding of strong thalamo-cortical coupling (Sarnthein et al., 2003, p. 65; Sarnthein et al., 2005, p. 114), we propose here an interpretation of the results in the framework of TCD. This thalamocortical concept of chronic neurogenic pain was proposed (Llinás *et al.*, 1999,2001; Jeanmonod *et al.*, 2001*b*) on the basis of experi-mental evidence (Llinás and Jahnsen, 1982; Ribary *et al.*, 1991; Steriade *et al.*, 1997; Steriade, 2001) and the clinical finding of LTS in pain patients (Lenz *et al.*, 1989; Jeanmonod *et al.*, 1993,1996). It may be characterized using the following sequential set of events (schematized in Fig. 7):

(i) A lesion leads to deafferentation of excitatory inputs on thalamic relay cells and initiates the neurogenic pain syndrome. The lesion may be peripheral or central and may lead to bottom–up deafferentation (Fig. 7A). A cortical lesion may lead to top–down deafferentation. The deafferentation of excitatory inputs results in dis-facilitation and cell membrane hyperpolarization.

(ii) In the hyperpolarized state, deinactivation of calcium T-channels causes thalamic relay neurons to fire LTS bursts at theta frequency (Llinás and Jahnsen, 1982).
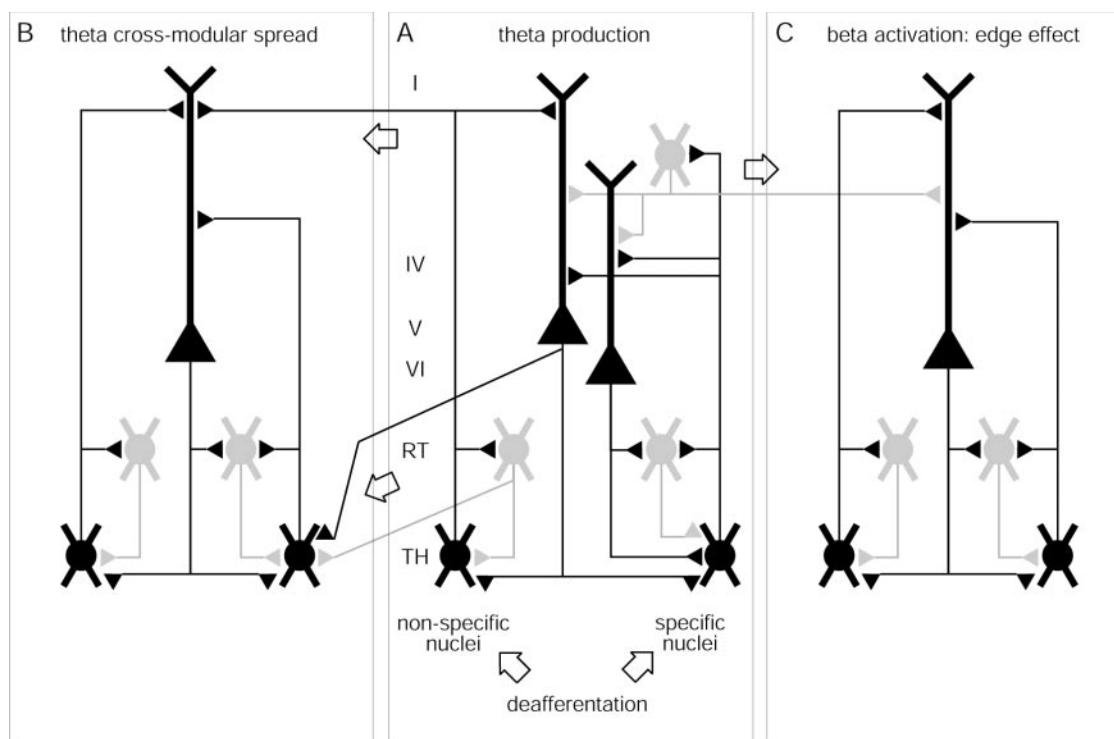

Fig. 7 Scheme of thalamocortical circuits relevant for TCD. Shown are three thalamocortical modules which we consider to be identical (Llinás *et al.*, 1999). Module A is depicted in more detail (Jones, 2001). One module includes, first, cortical layers (I, IV, V and VI) with pyramidal cells and one grey GABAergic inhibitory cell, second, nucleus reticularis (RT, grey GABAergic inhibitory cells) and third, thalamus (TH), represented by one specific and one non-specific cell. The specific thalamic cell projects to the apical dendrites of both layer V and VI pyramidal cells and collaterals sustain reticular feedback and cortical feedforward inhibitions. The non-specific thalamic cell projects to RT and only to the layer V pyramidal neuron but has a divergent connection onto the neighbouring module. The corticothalamic feedback connection is depicted as intramodular onto RT and its thalamic relay cell, and divergent intra- and cross-modular onto three thalamic relay cells. There are also divergent cross-modular reticulothalamic projections. The open arrows underline the cross-modular passages through thalamocortical, corticothalamic, reticulothalamic and corticocortical pathways. See the section discussion for details on the dynamics of the TCD.

Such hyperpolarization is thought to correlate with the state of reduced activity observed by PET in the thalamus of neurogenic pain patients (Iadarola *et al.*, 1995; Hsieh *et al.*, 1995; Nakabeppu *et al.*, 2001; Jones *et al.*, 2003).

(iii) Bursting thalamic relay neurons exert a rhythmic influence on thalamocortical loops in the theta frequency band. Thalamic and cortical areas are densely and reciprocally interconnected (Steriade *et al.*, 1997; Jones, 2001). The tight functional coupling between thalamus and cortex is confirmed by the high theta coherence between the two (Sarnthein *et al.*, 2003). This coupling is sustained by thalamocorticothalamic and also by thalamoreticulothalamic and corticoreticulothalamic recurrent projections (Steriade, 2001). The tendency of the thalamocortical network to maintain a given functional modality reinforces the hyperpolarized state over time (Pedroarena and Llinas, 1997).

(iv) Divergent thalamocortical, corticothalamic and reticulothalamic projections provide the anatomical substrate for diffusion of low frequency activity to an increasing number of neighbouring thalamocortical loops (Fig. 7B: theta cross-modular spread). This phenomenon may explain the often observed delay between the occurrence of the causal insult and the beginning of pain.

(v) After recruitment of a sufficiently large number of thalamocortical loops, excess theta power becomes measurable in thalamic local field potentials (Sarnthein *et al.*, 2003), MEG (Llinás *et al.*, 1999) and EEG (Fig. 1A). Why do we not observe a sharp EEG spectral peak at the LTS interburst frequency of 4 Hz? LTS exert influence on the thalamocortical system, but the same is true for cortical determinants of the EEG, such as refractory periods and axonal transmission latencies (Nunez *et al.*, 2001). Such determinants are not affected by the neurological disorders of our patients. This may explain why the presence of LTS in patients results in excess EEG oscillations spread over the whole theta band. Furthermore, increased low-frequency oscillations also occur during sleep (Steriade, 2001) and cognitive tasks (Klimesch, 1999; Kahana *et al.*, 2001), where they are considered as normal. It is the continuous and widespread overproduction of slow rhythms in the awake brain that characterizes TCD.

(vi) The final step towards the production of neurogenic pain is related to the reciprocal cortico-cortical inhibition mediated by GABAergic interneurons, which is a general feature of cortical organization (Fig. 7C). Thalamocortical modules in theta mode exert less collateral inhibition on neighbouring modules, which are thereby overactivated in high (beta) frequencies. This event has been termed edge effect (Llinás *et al.*, 1999). The concept is inspired by the effect of lateral inhibition in the retina. The asymmetrical inhibition between a low frequency cortical area and neighbouring high frequency domains provides a ring of reduced inhibition onto, and thus activation of, the cortex surrounding this low frequency

area. Support for such an effect was first provided by the increased interfrequency covariation between theta and beta ranges in MEG (Llinás et al., 2003; Llinás *et al.*, 2005). Recently, the increase of high frequency activation around a core of theta modules could be demonstrated in a slice preparation (Llinás, et al., 2003; Llinás et al., 2005). Also in the thalamus of patients, high interfrequency covariation and bicoherence was found (Sarnthein *et al.*, 2003). We were able to show enhanced bicoherence also in the scalp EEG from patients compared with healthy controls (Fig. 4). The dominance of beta activity in frontal electrodes (Fig. 3) also suggests anterior cortical generators of the scalp EEG, which we currently investigate and which would be consistent with activation of the insulae in the known cerebral network relevant for pain processing (Treede *et al.*, 1999; Jones *et al.*, 2003; Apkarian *et al.*, 2005).

Effect of CLT

The observed gradual change of the patients' EEG spectra towards the healthy control group spectrum has the following implications. First, it provides further support for our hypothesis that the amount of thalamic LTS burst production finds a correlate in the scalp EEG. Second, the gradual response to the sudden removal of LTS confirms that LTS activity constitutes only one of several determinants of EEG rhythmicity (Nunez *et al.*, 2001). Third, the EEG change over several months allows an estimate of the timeframe for wide range plasticity in the brain and parallels our observation of gradual clinical improvement (Jeanmonod *et al.*, 2001*a*).

Conclusions

Our data relate the clinical phenomenon of chronic neurogenic pain to slowed rhythmicity of scalp EEG. This relationship is further supported by the reduction of theta power in the EEG of patients after the therapeutic lesion CLT in the medial thalamus. The TCD mechanism offers an explanation of the pathophysiology in linking the function of calcium T-channels in the membrane of thalamic cells to the global properties of scalp EEG power spectra. EEG spectral analysis might in this way serve as an additional tool to diagnose chronic neurogenic pain and to monitor the postoperative development of patients.

Acknowledgements

References

Apkarian AV, Bushnell MC, Treede RD, Zubieta JK. Human brain mechanisms of pain perception and regulation in health disease. Eur J Pain 2005; 9: 463–84.

Berger H. Über das Elektroenkephalogramm des Menschen II. J Psychol Neurol 1930; 40: 160–79.

Delorme A, Makeig S. EEGLAB: an open source toolbox for analysis of single-trial EEG dynamics including independent component analysis. J Neurosci Methods 2004; 134: 9–21.

Dumermuth G, Huber PJ, Kleiner B, Gasser T. Analysis of the interrelations between frequency bands of the EEG by means of the bispectrum. A preliminary study. Electroencephalogr Clin Neurophysiol 1971; 31: 137–48.

Ebersole JS, Pedley TA. Current practice of clinical electroencephalography. Philadephia: Lippincott Williams & Wilkins; 2003.

Gücer G, Niedermeyer E, Long DM. Thalamic EEG recordings in patients with chronic pain. J Neurol 1978; 219: 47–61.

Hsieh JC, Belfrage M, Stone-Elander S, Hansson P, Ingvar M. Central representation of chronic ongoing neuropathic pain studied by positron emission tomography. Pain 1995; 63: 225–36.

Iadarola MJ, Max MB, Berman KF, Byas-Smith MG, Coghill RC, Gracely RH, et al. Unilateral decrease in thalamic activity observed with positron emission tomography in patients with chronic neuropathic pain. Pain 1995; 63: 55–64.

Jeanmonod D, Magnin M, Morel A. Thalamus and neurogenic pain: physiological, anatomical and clinical data. Neuroreport 1993; 4: 475–8.

Jeanmonod D, Magnin M, Morel A. Low-threshold calcium spike bursts in the human thalamus. Common physiopathology for sensory, motor and limbic positive symptoms. Brain 1996; 119: 363–75.

Jeanmonod D, Magnin M, Morel A, Siegemund M. Surgical control of the human thalamocortical dysrhythmia: I. Central lateral thalamotomy in neurogenic pain. Thalamus Relat Syst 2001a; 1: 71–9.

Jeanmonod D, Magnin M, Morel A, Siegemund M, Cancro R, Lanz M, et al. Thalamocortical dysrhythmia II. Clinical and surgical aspects. Thalamus Relat Syst 2001b; 1: 245–54.

Jones EG. The thalamic matrix and thalamocortical synchrony. Trends Neurosci 2001; 24: 595–601.

Jones AK, Kulkarni B, Derbyshire SW. Pain mechanisms and their disorders. Br Med Bull 2003; 65: 83–93.

Kahana MJ, Seelig D, Madsen JR. Theta returns. Curr Opin Neurobiol 2001; 11: 739–44.

Klimesch W. EEG alpha and theta oscillations reflect cognitive and memory performance: a review and analysis. Brain Res Brain Res Rev 1999; 29: 169–95.

Landolt HP, Retey JV, Tonz K, Gottselig JM, Khatami R, Buckelmuller I, et al. Caffeine attenuates waking and sleep electroencephalographic markers of sleep homeostasis in humans. Neuropsychopharmacology 2004; 29: 1933–9.

Lenz FA, Kwan HC, Dostrovsky JO, Tasker RR. Characteristics of the bursting pattern of action potentials that occurs in the thalamus of patients with central pain. Brain Res 1989; 496: 357–60.

Lindhardt K, Gizurarson S, Stefansson SB, Olafsson DR, Bechgaard E. Electroencephalographic effects and serum concentrations after intranasal and intravenous administration of diazepam to healthy volunteers. Br J Clin Pharmacol 2001; 52: 521–7.

Llinás R, Jahnsen H. Electrophysiology of mammalian thalamic neurones in vitro. Nature 1982; 297: 406–8.

Llinás RR, Ribary U, Jeanmonod D, Kronberg E, Mitra PP. Thalamocortical dysrhythmia: a neurological and neuropsychiatric syndrome characterized by magnetoencephalography. Proc Natl Acad Sci USA 1999; 96: 15222–7.

Llinás R, Ribary U, Jeanmonod D, Cancro R, Kronberg E, Schulman J, et al. Thalamocortical dysrhythmia I. Functional and imaging aspects. Thalamus Relat Syst 2001; 1: 237–44.

Llinas RR, Leznik E, Urbano FJ. Temporal binding via cortical coincidence detection of specific and nonspecific thalamocortical inputs: a voltage-dependent dye-imaging study in mouse brain slices. Proc Natl Acad Sci USA 2002; 99: 449–54.

Llinas R, Urbano FJ, Leznik E, Ramirez RR, van Marle HJ. Rhythmic and dysrhythmic thalamocortical dynamics: GABA systems and the edge effect. Trends Neurosci 2005; 28: 325–33.

McEvoy LK, Pellouchoud E, Smith ME, Gevins A. Neurophysiological signals of working memory in normal aging. Brain Res Cogn Brain Res 2001; 11: 363–76.

Morel A, Magnin M, Jeanmonod D. Multiarchitectonic and stereotactic atlas of the human thalamus. J Comp Neurol 1997; 387: 588–630.

Nakabeppu Y, Nakajo M, Gushiken T, Tsuchimochi S, Tani A, Kanmura Y. Decreased perfusion of the bilateral thalami in patients with chronic pain detected by Tc-99m-ECD SPECT with statistical parametric mapping. Ann Nucl Med 2001; 15: 459–63.

Niedermeyer E, Lopes da Silva FH. Electroencephalography: basic principles, clinical applications, and related fields. Philadephia: Lippincott Williams & Wilkins; 1999.

Nunez PL, Wingeier BM, Silberstein RB. Spatial-temporal structures of human alpha rhythms: theory, microcurrent sources, multiscale measurements, and global binding of local networks. Hum Brain Mapp 2001; 13: 125–64.

Pedroarena C, Llinas R. Dendritic calcium conductances generate high-frequency oscillation in thalamocortical neurons. Proc Natl Acad Sci USA 1997; 94: 724–8.

Percival DB, Walden AT. Spectral analysis for physical applications. Cambridge: Cambridge University Press; 1993.

Peyron R, Laurent B, Garcia-Larrea L. Functional imaging of brain responses to pain. A review and meta-analysis (2000). Neurophysiol Clin 2000; 30: 263–88.

Pfurtscheller G, Stancak A Jr, Neuper C. Event-related synchronization (ERS) in the alpha band—an electrophysiological correlate of cortical idling: a review. Int J Psychophysiol 1996; 24: 39–46.

Ribary U, Ioannides AA, Singh KD, Hasson R, Bolton JP, Lado F, et al. Magnetic field tomography of coherent thalamocortical 40-Hz oscillations in humans. Proc Natl Acad Sci USA 1991; 88: 11037–41.

Salinsky MC, Oken BS, Morehead L. Test-retest reliability in EEG frequency analysis. Electroencephalogr Clin Neurophysiol 1991; 79: 382–92.

Salinsky MC, Oken BS, Storzbach D, Dodrill CB. Assessment of CNS effects of antiepileptic drugs by using quantitative EEG measures. Epilepsia 2003; 44: 1042–50.

Sarnthein J, Morel A, von Stein A, Jeanmonod D. Thalamic theta field potentials and EEG: high thalamocortical coherence in patients with neurogenic pain, epilepsy and movement disorders. Thalamus Relat Syst 2003; 2: 231–8.

Sarnthein J, Morel A, von Stein A, Jeanmonod D. Thalamocortical theta coherence in neurological patients at rest and during a working memory task. Int J Psychophysiol 2005; 57: 87–96.

Schack B, Vath N, Petsche H, Geissler HG, Möller E. Phase-coupling of theta-gamma EEG rhythms during short-term memory processing. Int J Psychophysiol 2002; 44: 143–63.

Steriade M. Impact of network activities on neuronal properties in corticothalamic systems. J Neurophysiol 2001; 86: 1–39.

Steriade M, Jones EG, McCormick DA. Thalamus: organisation and Function. Vol. 1. Oxford: Elsevier; 1997.

Treede RD, Kenshalo DR, Gracely RH, Jones AK. The cortical representation of pain. Pain 1999; 79: 105–11.